

Saw-Tooth Chip Formation and Its Effect on Cutting Force Fluctuation in Turning of Inconel 718

Song Zhang^{1#}, Jianfeng Li¹, Xiaoli Zhu^{1,2}, and Honggang Lv¹

¹ Key Laboratory of High Efficiency and Clean Mechanical Manufacture (Ministry of Education), School of Mechanical Engineering, Shandong University, Jinan 250061, China
² Shelfoil Petroleum Equipment & Services Co., Ltd, Dezhou 253034, China

Corresponding Author / E-mail: zhangsong@sdu.edu.cn, TEL, FAX: +86-531-88392746

KEYWORDS: Saw-tooth chip formation, Cutting force fluctuation, Frequency analysis, Inconel 718, Turning

Chip formation and its morphology are important features of metal cutting, and they can yield much more important information on the cutting operations. Meantime, the cutting forces are the most commonly used on-line indicators to monitor the cutting process. In this research, the formation of the saw-tooth chips has been investigated in association with the fluctuation of the cutting force components under different cutting parameters in turning of Inconel 718 with (Ti, Al)N/TiN coated cutting tools under dry cutting condition. By means of the optical microscopy and the scanning electron microscopy (SEM), the saw-tooth chips are observed at high cutting speeds, which directly cause the cutting force components to fluctuate. Based on the frequency analysis, the segmentation frequencies of the saw-tooth chips and the fluctuation frequency of the cutting forces are very close to each other. It indicates that the formation of the saw-tooth chips is one of the important factors leading to the periodical fluctuation of the cutting force components, even though the cutting parameters all keep constant in turning of Inconel 718.

Manuscript received: September 21, 2012 / Accepted: March 14, 2013

1. Introduction

There is an increasing demand for critical aerospace and aeronautic components, in particular in the hot sections of the gas turbine engines, which are made from nickel-based superalloys primarily due to their high strength-to-weight ratio, high corrosion resistance, and high-temperature strength.¹ Among the nickel-based superalloys, Inconel 718 is the most extensively used alloy; however, Inconel 718 usually shows poor machinability due to its low thermal conductivity, high hardness at the elevated temperature, and high chemical affinity with many cutting tool materials.² These above-mentioned characteristics cause cutting temperature and resultant tool damage to increase even at low cutting speed and low feed rate. The difficulty of machining Inconel 718 resolves itself into the following basic problems: short tool life, low productivity, and severe surface damages extending to subsurface levels.^{3,4} Therefore, it is essential to investigate and understand the cutting mechanism in order to meet the increasing demands for higher manufacturing efficiency and machining quality, as well as lower manufacturing cost.

The chip formation is the heart of metal cutting processes, which is determined by the combined effects of many process parameters and

has served an important role in revealing the mechanics of metal removal and the important friction phenomena occurring in cutting processes.⁵ From the point of view of controlling and optimizing the cutting operations, the effects of cutting parameters, and the interaction between the cutting tool and work material on chip formation process is of great interest.^{6,7} Therefore, the adequate understanding of the chip formation and chip-breaking is needed if improvement and better utilization of machining is to be achieved.⁸ The saw-tooth chips are normally produced during machining nickel-based superalloys.^{9,10} Saw-tooth chip formation is generally believed to be due to either the ‘crack theory’ or the ‘adiabatic shear theory’.^{11,12} Sun et al.¹³ demonstrated that the peak of the cyclic force when producing saw-tooth chips was larger than that producing the continuous chip. The formation of the saw-tooth chips is the source of cutting force components fluctuation and serious vibration, which directly limit material removal rate and, consequently, productivity.¹⁴ Moreover, the thermo-mechanical behavior at the workpiece/tool interface can be contributed by changes in the chip formation process, which in turn results in the premature tool failure and deteriorates the machining quality.^{15,16}

The increasing demands for higher manufacturing efficiency have resulted in a great deal of researches aimed at cutting processes

monitoring. Among the indirect on-line monitoring methods, the cutting force signal is the most commonly used variable as a cutting process indicator, which can provide valuable information related to tool wear, and surface texture and accuracy of a workpiece.¹⁷ Clarifying the mechanism and factors responsible for saw-tooth chip formation and exploring the relationship between the formation of saw-tooth chips and the cutting force fluctuation is of great importance to the development of an effective cutting process monitoring strategy. So far, very few published articles explore the correlation between the formation of the saw-tooth chips and the dynamic fluctuation of the cutting force components in turning of nickel-based alloys. This research aims to increase the understanding of the saw-tooth chip formation mechanism and its influence on the fluctuation of the cutting force components in terms of the frequency analysis during turning Inconel 718.

2. Experimental Work

2.1 Experimental design

As shown in Table 1, three cutting parameters (cutting speed v , feed

Table 1 Cutting parameters and their levels

Cutting parameters	Levels				
	1	2	3	4	5
Cutting speed v (m/min)	30	35	40	45	50
Feed rate f (mm/rev)	0.08	0.12	0.16	0.2	0.24
Depth of cut a_p (mm)	0.2	0.5	0.8	1.1	1.4

Table 2 Experimental design based on Taguchi's technique

Experiment number	Cutting parameters		
	v (m/min)	f (mm/rev)	a_p (mm)
1	30	0.08	0.2
2	30	0.12	0.5
3	30	0.16	0.8
4	30	0.20	1.1
5	30	0.24	1.4
6	35	0.08	0.5
7	35	0.12	0.8
8	35	0.16	1.1
9	35	0.20	1.4
10	35	0.24	0.2
11	40	0.08	0.8
12	40	0.12	1.1
13	40	0.16	1.4
14	40	0.20	0.2
15	40	0.24	0.5
16	45	0.08	1.1
17	45	0.12	1.4
18	45	0.16	0.2
19	45	0.20	0.5
20	45	0.24	0.8
21	50	0.08	1.4
22	50	0.12	0.2
23	50	0.16	0.5
24	50	0.20	0.8
25	50	0.24	1.1

rate f and depth of cut a_p) were selected as the independent factors in turning of Inconel 718. The ranges of the cutting parameters were determined according to the tool manufacturer's recommended values (Seco Tools Company) and the literatures.^{4,6,9} Each cutting parameter had five levels, which were denoted by '1', '2', '3', '4', and '5', respectively. Based on Taguchi's technique, a standard L_{25} (5^3) orthogonal array was designed as shown in Table 2.

2.2 Workpiece material, machine tool and cutting tool

Inconel 718 alloy cylinders, 60 mm in diameter and 300 mm in length were prepared for the turning experiments. The chemical compositions and typical mechanical properties of the workpiece material are given in Tables 3 and 4, respectively. Before turning experiments, the exterior surfaces of the specimen were turned to remove the original oxidation layers and other defaults.

In this research, all the turning experiments were carried out on a CA6140 lathe machine with one coated carbide insert TNMG160408 mechanically clamped on a tool-holder STGCR 2525M16 (Seco Tools Company). No cutting fluids were used during turning process. The indexable inserts were deposited by PVD (physical vapor deposition) process with the thin multilayer (Ti, Al)N/TiN coatings. Fig. 1 shows the geometrical information about the tool-holder and the indexable insert used in the turning experiments. The combination of the indexable insert and the tool-holder resulted in the rake angle $\gamma_0 = -6^\circ$, and the clearance angle $\lambda_s = -6^\circ$.

2.3 Experimental procedure

The cutting force acting on a cutting tool (Fig. 2) can be dissolved into three components, i.e., feed force F_f , thrust force F_p , and tangential

Table 3 Chemical compositions of Inconel 718

Element	Content (wt%)
Ni + Co	50 - 55
Cr	17 - 21
Fe	Balance
Nb + Ta	4.75 - 5.5
Mo	2.8 - 3.3
Ti	0.65 - 1.15
Al	0.2 - 0.8

Table 4 Typical mechanical properties of Inconel 718 at room temperature

Tensile strength (MPa)	Yield strength (MPa)	Young's modulus (GPa)	Hardness (HRC)
1240	1036	206	36

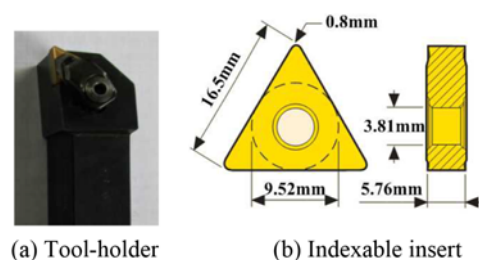


Fig. 1 Geometries of the tooling system

force F_c , respectively. As shown in Fig. 3, the three cutting force components were real-time measured using the Kistler piezoelectric dynamometer (Type 9441) mounted on the lathe. The charge generated at the dynamometer was amplified using an amplifier (Type 5807). The amplified signals from the charge amplifier were fed to the data acquisition system (Type AZ208R) where they were converted to the digital output, and subsequently stored in the computer.

The free and back surfaces of the collected chips under different cutting parameters were examined under the scanning electron microscope (Hitachi, S-2500). In order to analyze the chip characteristics further, the collected chips were mounted with epoxy, in which the free and back surfaces of the chip both located perpendicularly to the resin surface. The chip specimens were then ground and polished perpendicular to the axis of the cylinder until mirror-like surfaces were obtained. The polished chip specimens were subsequently observed under the digital optical microscope (Keyence, VHX-600E).

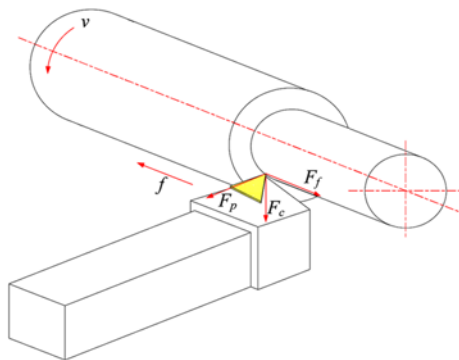
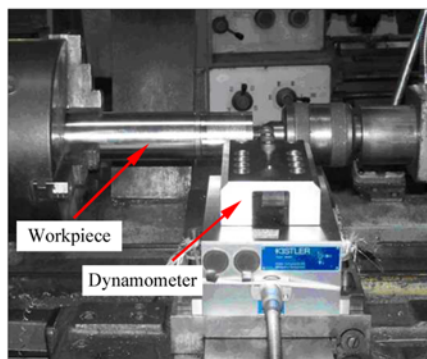
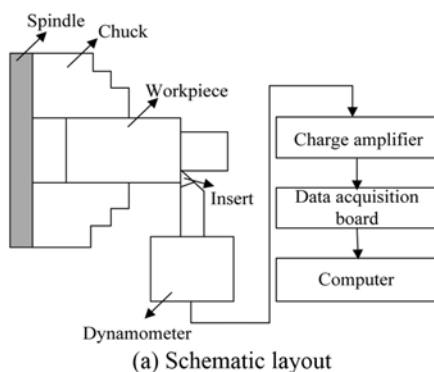


Fig. 2 Schematic of cutting force components



(b) Cutting force dynamometer

Fig. 3 Experimental setup

3. Results and Discussions

3.1 Chip morphology

The chip morphology is an important aspect which is commonly considered to evaluate the performance of the cutting operations. The chip types are determined by the combined effects of type of cut (continuous or intermittent cut), work material properties, cutting tool geometry, cutting parameters, cutting fluids (type of fluids and method of applications), and other factors. The chips produced under the cutting parameters given in Table 1 can be basically divided into three categories, i.e., the washer type chip (Figs. 4(a) and 4(c)), the elemental chip (Fig. 4(d)), and the ribbon chip (Fig. 4(b)), respectively.

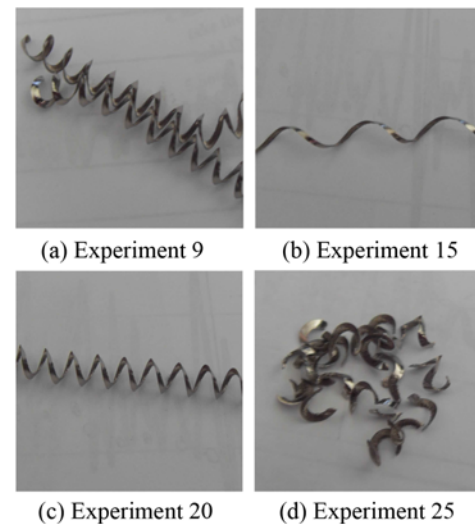
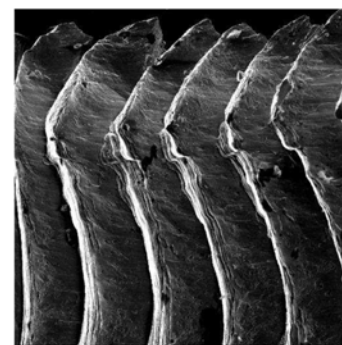
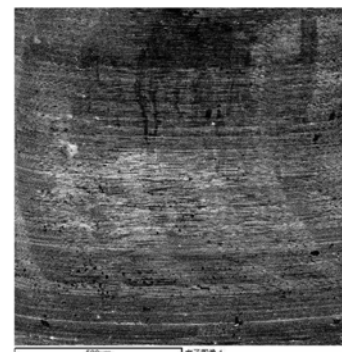


Fig. 4 Representative chips under different cutting parameters



(a) Free surface



(b) Back surface

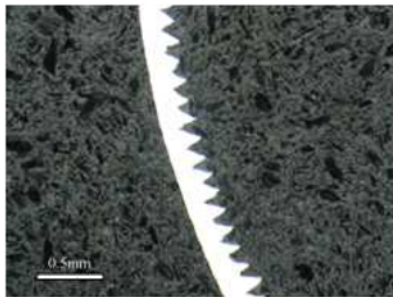
Fig. 5 Surface topography of the chip (Experiment 20)

Under the scanning electron microscope (SEM), the lamella structures at the free surface of the collected chips have been observed. These lamellas, which are normal to the direction of chip flow, extend across the width of the chips (Fig. 5(a)). The free surface of the chip generally tends to transfer from the relatively fine and uniform lamella structures to the large structures with the increase of cutting speed and the undeformed chip thickness (depth of cut). The larger lamella structures in terms of width and depth usually indicate that the formation of the classical continuous fragmentary chips with the saw tooth, which suggests that the presence of the lamella structures on the free surface of the chips is the evidence of the shear localization.¹⁸

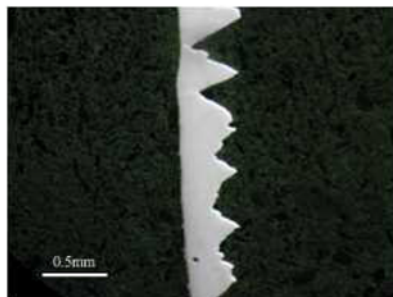
As shown in Fig. 5(b), due to the strong friction between the back surface of the chips and the rake surface of the cutting tool, some



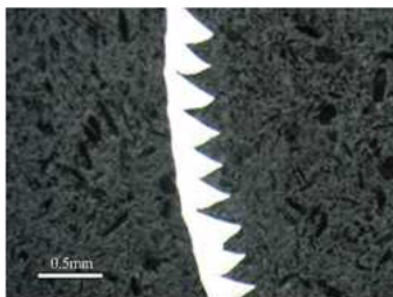
(a) Experiment 9



(b) Experiment 15



(c) Experiment 20



(d) Experiment 25

Fig. 6 Cross-sections of chips under different cutting speeds

stripes parallel to each other appear on the back surface. However, compared with the free surface, the back surface of the chips are much smoother and shinier. This phenomenon is attributed to the high contact stresses and the high shear stresses at the tool-chip interface.

The chip morphology varies with the combination of cutting parameters; however, as reported by Thakur et al.¹⁹ saw-tooth is a characteristic type of the chips when machining nickel-based alloys at high cutting speed. Accordingly, only saw-tooth chips were chosen for morphology investigation. To further analyze the effect of the cutting parameters on the chip morphology, several cross-sections of the saw-tooth chips were made and the corresponding optical images are presented in Fig. 6. Some very fine and irregular saw teeth are observed at the chip cross-section at low cutting speed; while the saw-tooth phenomenon becomes more obvious and results in the reduction of its segmentation frequency at high cutting speed. It indicates that the higher the cutting speed, the more noticeable the saw-tooth chips, which may be attributed to the cyclic crack formation at the free surface of the chip. Crack initiation and shear localization under high shear deformation at high cutting speeds lead to the catastrophic failure within the upper region of the primary shear zone.

3.2 Chip segmentation frequency

Based on the cross-section of the saw-tooth chip in Fig. 7, the tooth pitch p_c (saw-to-saw distance), the tooth height chip h (distance from the peak to the valley of the chip) of the saw-tooth chip were respectively measured at different locations to investigate the geometrical characteristics of saw-tooth cross-section of the chips during turning Inconel 718.

By considering a mean sliding speed of the chip on the tool rake surface of the cutting tool and the mean tooth pitch between two shearing planes in the periodic segmented chip region (Fig. 7), the segmentation frequency of the saw-tooth chips may be found as follows:

$$f_{\text{chip}} = \frac{1000}{60} \cdot \frac{v_c}{p_c} = r \cdot \frac{1000}{60} \cdot \frac{v}{p_c} \quad (1)$$

where f_{chip} - the chip segmentation frequency determined from the chip geometry (Hz), v_c - the mean sliding speed of the chip on the rake surface of the cutting tool (m/min), p_c - the saw-tooth pitch between two shearing planes (mm), v - cutting speed (mm/min), and r - the cutting ratio for the chip.

Microscopic measurements on the replica revealed that the mean

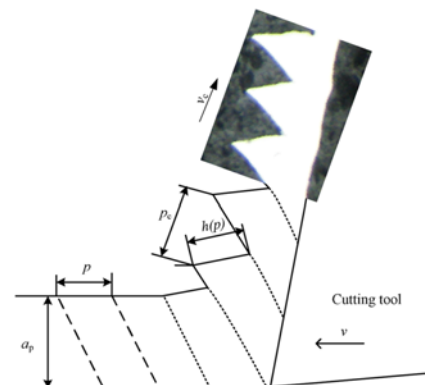


Fig. 7 Saw-tooth chip geometry

distance between the peak and the valley on the free surface of the chip corresponded to the mean distance between cracks on the workpiece surface p .²⁰ Therefore, a convenient method of finding r is to divide the mean tooth pitch (p_c) by the mean value of tooth height h ($=p$). Thus, the cutting ratio r is

$$r = \frac{v_c}{v} = \frac{p_c}{p} \quad (2)$$

where p - mean distance between cracks on the workpiece surface (μm), and h - mean value of tooth height (μm).

Substituting Eq. (2) into Eq. (1), the segmentation frequency of the saw-tooth chips can be modified as follows,

$$f_{\text{chip}} = \frac{v}{p} \quad (3)$$

where f_{chip} - segmentation frequency of saw-tooth chips (Hz).

Taking the saw-tooth chip in Fig. 6(a) for example, based on the average value of the tooth height h of the chip measured at the three different positions and cutting speed v (35 m/min), the mean segmentation frequency of the saw-tooth chip is about 4667 Hz.

Similarly, according to the cross-section geometrical information in Figs. 6(b), 6(c) and 6(d), the other segmentation frequencies of the saw-tooth chips can also be calculated and are given in Table 5. With the increase of cutting speed, the segmentation frequency of saw-tooth chip decreases, and the tendency of saw-tooth chip formation becomes more and more noticeable.

Table 5 Segmentation frequency of saw-tooth chips

Experiment number	9	15	20	25
Frequency f_{chip} (Hz)	4667	4400	3472	3333

3.3 Fluctuation frequency of cutting forces

Once the saw-tooth chip forms in turning of Inconel 718, the chip thickness will periodically change. The shear angle dominates cutting behavior. Theoretically, increasing the chip thickness can decrease the shear angle, leading to the increase of cutting force,²¹ and vice versa. Accordingly, as shown in Fig. 8, along with the formation of the saw-tooth chips the magnitudes of the three force components are not constant even though the cutting parameters (cutting speed v , feed rate f_s and depth of cut a_p) all keep constant. From the real-time signals for three cutting force components, it can be seen that the cutting force components basically appear periodical fluctuation.

The cutting time T in microseconds (ms) between the two cutting force peaks in Fig. 8(c) can be expressed by the following equation:

$$T = \frac{\sum t}{10} = \frac{2.85}{10} = 0.28(\text{ms}) \quad (4)$$

where T - cutting time between two cutting force peaks (ms), $\sum t$ - total time between 11 cutting force peaks (ms).

Thus, the fluctuation frequency of the cutting forces in Fig. 8 can be calculated as follows,

$$f_{\text{force}} = \frac{1}{T} = \frac{1}{0.285 \times 10^{-3}} = 3508(\text{Hz}) \quad (5)$$

where f_{force} - fluctuation frequency of cutting forces (Hz).

Analysis of the cutting force data reveals that the fluctuation frequency of the cyclic cutting force is about 3508 Hz. Similarly, the fluctuation frequencies of the cutting force components in other groups

Table 6 Fluctuation frequency of cutting forces

Experiment number	9	15	20	25
Frequency f_{force} (Hz)	4725	4647	3589	3508

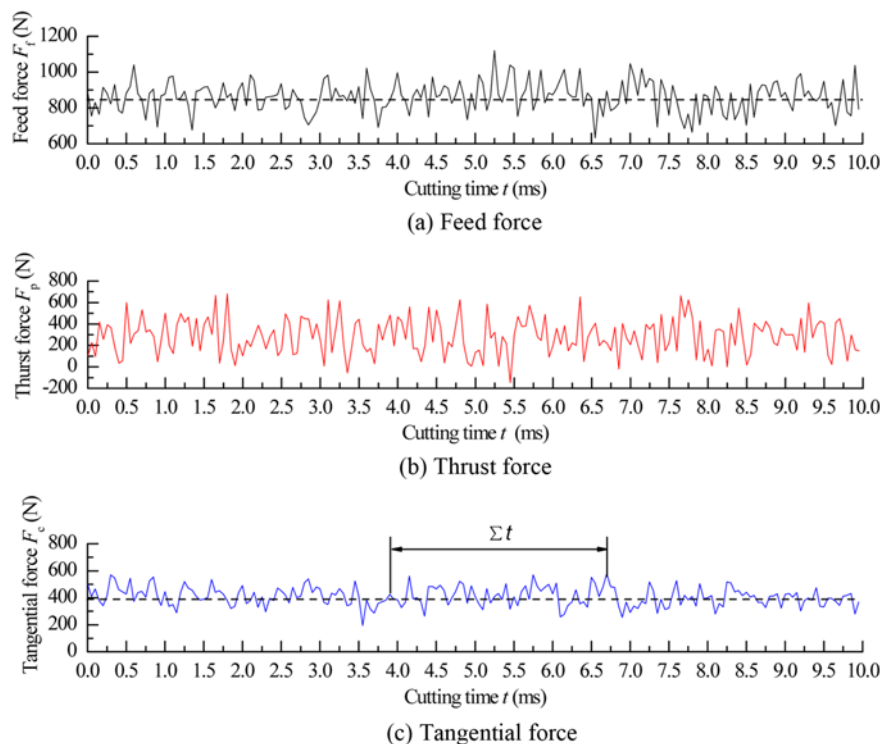


Fig. 8 Real-time signal of cutting force components

are given in Table 6. The periodical fluctuation of the cutting force components can be attributed to the variation of the chip thickness when the saw-tooth chips produced at higher cutting speeds.

3.4 Correlation between saw-tooth chip and cutting force variation

Comparing Table 5 with Table 6, it can be found that the fluctuation frequency of the cyclic cutting force components agrees very well with the segmentation frequency of the saw-tooth chips, indicating that the cyclic cutting forces fluctuation is mainly caused by the saw-tooth chip formation process. This agrees with the previously established correlation between the segmentation frequency of the saw-tooth chips and the cyclic force frequency obtained by the other researchers.²² Moreover, the higher frequency of saw-tooth chip formation, the higher fluctuation frequency of the cutting forces is obtained.

As mentioned above, the formation of the saw-tooth chips is the source of cutting force components fluctuation and serious vibration, which is detrimental to the stability of the whole machining system; more important, during turning Inconel 718 the formation of the saw-tooth chips is very difficult to be avoided. Therefore, it is essential to select the proper cutting tools and machine tools with high stiffness to improve the dynamic performances of the machining system. Consequently, machining quality and productivity of turning Inconel 718 can be also guaranteed.

4. Conclusions

In the present work the saw-tooth chip formation and its effect on the fluctuation of the cutting force components have been studied when turning Inconel 718 using (Ti, Al)N/TiN coated cutting tools under dry cutting condition. Based on the findings of this study, the following conclusions are drawn as follows,

- (1) The saw-tooth chips due to the cyclic crack formation at the free surface of the chip are observed at high cutting speed.
- (2) The periodical variation of the chip thickness causes the fluctuation of the cutting force components even though the cutting parameters all keep constant during turning process.
- (3) The segmentation frequency of the saw-tooth chips and the fluctuation frequency of cutting forces are very close to each other. It indicates that the formation of the saw-tooth chips is the most important factor influencing the periodical fluctuation of the cutting force components in turning of Inconel 718.

ACKNOWLEDGEMENTS

This work has been supported by “High-end CNC Machine Tools and Basic Manufacturing Equipments” National Science and Technology Major Project (Grant No. 2012ZX04006011), and Taishan Scholar Program Foundation of Shandong, P. R. China.

REFERENCES

1. Dudzinsk, D., Devillez, A., Moufki, A., Larrouquere, D., Zerrouki, V., and Vigneau, J., “A review of developments towards dry and high speed machining of Inconel 718 alloy,” *Int. J. Mach. Tools Manuf.*, Vol. 44, pp. 439-456, 2004.
2. Kitagawa, T., Kubo, A., and Maekawa, K., “Temperature and wear of cutting tools in high-speed machining of Inconel 718 and Ti-6Al-6V-2Sn,” *Wear*, Vol. 202, pp. 142-148, 1997.
3. Vagnorius, Z. and Sørb, K., “Effect of high-pressure cooling on life of SiAlON tools in machining of Inconel 718,” *Int. J. Adv. Manuf. Technol.*, Vol. 54, pp. 83-92, 2011.
4. Pawade, S. R. and Joshi, S. S., “Multi-objective optimization of surface roughness and cutting forces in high-speed turning of Inconel 718 using Taguchi grey relational analysis (TGRA),” *Int. J. Adv. Manuf. Technol.*, Vol. 56, pp. 47-62, 2011.
5. Ning, L., Veldhuis, S. C., and Yamamoto, K., “Investigation of wear behavior and chip formation for cutting tools with nano-multilayered TiAlCrN/NbN PVD coating,” *Int. J. Mach. Tools Manuf.*, Vol. 48, pp. 656-665, 2008.
6. Thakur, D. G., Ramamoorthy, B., and Vijayaraghavan, L., “Machinability investigation of Inconel 718 in high-speed turning,” *Int. J. Adv. Manuf. Technol.*, Vol. 45, pp. 421-429, 2009.
7. Thakur, D. G., Ramamoorthy, B., and Vijayaraghavan, L., “A study on the parameters in high-speed turning of superalloy Inconel 718,” *Mater. Manuf. Process.*, Vol. 24, pp. 497-503, 2009.
8. Güllü, A. and Karabulut, Ş., “Dynamic chip breaker design for Inconel 718 using positive angle tool holder,” *Mater. Manuf. Process.*, Vol. 23, pp. 852-857, 2008.
9. Siemers, C., Zahra, B., Ksiezzyk, D., Rokicki, P., Spatz, Z., Fusova, L., Rosler, J., and Saksl, K., “Chip formation and machinability of nickel-base superalloys,” *Adv. Mater. Res.*, Vol. 278, pp. 460-465, 2011.
10. Pawadea, R. S. and Joshia, S. S., “Mechanism of chip formation in high-speed turning of Inconel 718,” *Mach. Sci. Technol.*, Vol. 15, pp. 132-152, 2011.
11. Vyas, A. and Shaw, M. C., “Mechanics of saw-tooth chip formation in metal cutting,” *ASME, J. Manuf. Sci. Eng.*, Vol. 211, pp. 163-172, 1999.
12. Barry, J., Byrne, G., and Lennon, D., “Observations on chip formation and acoustic emission in machining Ti-6Al-4V alloy,” *Int. J. Mach. Tools Manuf.*, Vol. 41, pp. 1055-1070, 2001.
13. Aruna, M., Dhanalakshmi, V., and Mohan, S., “Wear analysis of ceramic cutting tools in finish turning of Inconel 718,” *Int. J. Eng. Sci. Technol.*, Vol. 2, pp. 4253-4262, 2010.
14. Mian, A. J., Driver, N., and Mativenga, P. T., “Chip formation in microscale milling and correlation with acoustic emission signal,” *Int. J. Adv. Manuf. Technol.*, Vol. 56, pp. 63-78, 2011.
15. Kang, I. S., Kim, J. H., Hong, C., and Kim, J. S., “Development and evaluation of tool dynamometer for measuring high frequency cutting forces in micro milling,” *Int. J. Precis. Eng. Manuf.*, Vol. 11,

- No. 6, pp. 817-821, 2010.
16. Shaw, M. C., "A new mechanism of plastic flow," *Int. J. Mech. Sci.*, Vol. 22, pp. 673-686, 1980.
 17. Thakur, D. G., Ramaoorthy, B., and Vijayaraghavan, L., "Study on the machinability characteristics of superalloy Inconel 718 during high speed turning," *Mater. Des.*, Vol. 30, pp. 1718-1725, 2009.
 18. Shaw, M. C., "Metal cutting principles (2nd edition)," Oxford University Press, pp. 544-551, 2005.
 19. Xie, J., Luo, M. J., He, J. L., Liu, X. R., and Tan, T. W., "Micro-grinding of micro-groove array on tool rake surface for dry cutting of titanium alloy," *Int. J. Precis. Eng. Manuf.*, Vol. 13, No. 10, pp. 1845-1852, 2012.
 20. Vyas, A. and Shaw, M. C., "Mechanics of saw-tooth chip formation in metal cutting," *ASME, J. Manuf. Sci. Eng.*, Vol. 211, pp. 163-172, 1999.